2017

Dye-sensitised Solar Cell Antenna

Oisin O'Conchubhair
Technological University Dublin

Patrick McEvoy
Technological University Dublin, patrick.mcevoy@tudublin.ie

Max Ammann
Technological University Dublin, max.ammann@tudublin.ie

Recommended Citation

O'Conchubhair, O., McEvoy, P., Ammann, M. (2017). Dye-sensitised solar cell antenna. IEEE Antennas and Wireless Propagation Letters, vol.16, pp.352 - 355. doi:10.1109/LAWP.2016.2576687

Dye-Sensitised Solar Cell Antenna

Oisin O'Conchubhair, Patrick McEvoy, *Senior Member, IEEE* and Max J. Ammann, *Senior Member, IEEE*

***Abstract*— Dye-sensitised solar cells are proposed as a solar-antenna in the form of a proof-of-concept dipole operating at 1.1 GHz. Comprised of glass plates in basic rectangular shapes, various material properties are considered for impact on antenna performance at three phases of assembly. Simulated and empirical analyses indicate how such low-cost solar cells can also realise viable concurrent antenna designs.**

***Index Terms*— Dipole Antenna, Dye-sensitised Solar Cell.**

I. Introduction

INTEGRATED solar cell antennas for wireless applications combine a solar power generator with the radiating element in a compact device to reduce battery maintenance costs [1, 2].

Silicon (Si) solar cells used indoors are outperformed by dye-sensitised (DS) solar cells which benefit from wider acceptance angles and better absorption capacity for diffuse sunlight and fluorescent light [3]. While crystalline Si-cells are more efficient, DS-cells are cheaper and can be printed on flexible conductive plastic layers for enhanced integration. Indoor use mitigates risk of excessive expansion of liquid electrolytes and packaging fracture due to extreme temperatures. DS-cells also support power storage capabilities which could eliminate requirements for a battery [4].

Integration criteria for dye-sensitised solar antennas differ from those using different solar cells. A copper dipole printed on FR-4 substrate was suspended over a 3 W polycrystalline-Si cell ground plane which supported the feed line and acted as an antenna reflector [5]. While it had sufficient power for a wireless sensor, the need to suspend the dipole over the polycrystalline-Si cell resulted in a larger volume which inhibited indoor use. The radiating elements of a folded dipole antenna comprised of emitter-wrap-through silicon (EWT-Si) cells and a solar concentrator acted as the reflector [6]. The concentrator contributed to a high 11.1 dBi gain and to the EWT-Si cell generating 73.7 mW under a 1,000 W/m^2 light source. Similarly, the reflector produced a large volume with a directive radiation pattern to limit indoor use. A 3 - 10 GHz ultra-wideband dipole was made using amorphous-Si (a-Si) cells and generated 0.04 W under a 1,000 W/m^2 light source [7]. While the significantly smaller design avoided a large ground plane reflector, a-Si-cells are 14% less efficient than DS-cells [8].

Design of viable solar antennas takes account of impact on the radiating performance due to semi-conductor, dielectric or metallic properties of the solar cells. Varied orientation of a patch antenna over the anode lattice of a polycrystalline Si-cell resulted in differing levels of exposure to the lossy silicon, frequency shifts and gain reduction [9]. Radiation coupling between a crossed-slot antenna and a panel of a-Si-cells [10] hosted on an antenna ground plane was minimised by optimising the cell area while simultaneously reducing the solar footprint. Since the solar performance of a DS-cell avoids metallic lattices, the radiating performance should be less sensitive to material coupling and anisotropy.

The feasibility of designing a DS-cell solar antenna for small, unobtrusive devices is reported using a proof-of-concept dipole to form a toroidal radiation pattern while simultaneously harvesting light energy from front and rear surfaces. In this instance, the solar antenna design was constrained to 1.1 GHz due to the 20 × 40 mm dimensions of the glass slides available for prototype packaging of the Indium Tin Oxide (ITO). A co-planar feed and balun provided a series connection between the two solar cell dipole elements. In an applied design, a smaller balanced transceiver circuit could feed an antenna directly. Additionally, an RF choke comprising discrete components would make the DC contacts at the outer edges of the antenna appear as open circuits at the antennas resonant frequency, thus isolating the DC load from the RF circuit [1].

Three design stages of the solar cell were investigated; (1) a dipole made from ITO slides, (2) a dipole made from ITO slides with a layer of Titanium Dioxide (TiO_2) and (3) a dipole made from complete DS-cells. A copper dipole of identical dimensions was used for reference.

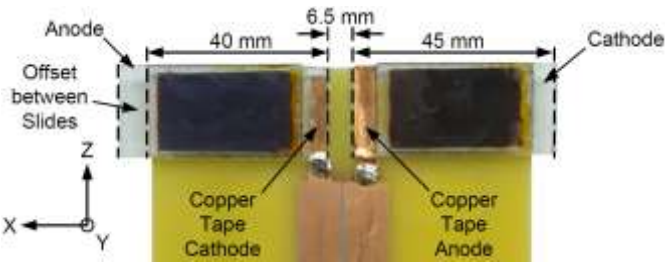

Fig. 1 – Rear of dye-Sensitised Solar Dipole Antenna

Manuscript received March 31, 2016; revised May 12, 2016; accepted June 02 2016. Date of publication **Month XX**, 201**X**; date of current version **Month XX**, 201**X**. This work was part funded by the Irish Higher Education Authority under PRTLI Cycle 5 as part of the Telecommunication Graduate Initiative and by SFI under TIDA 14/TIDA/2479. O. O'Conchubhair, P. McEvoy and M. J. Ammann are with the Antenna & High Frequency Research Centre, School of Electrical and Electronic Engineering, Dublin Institute of Technology, Kevin Street, Dublin D08 NF82, Ireland (e-mail: **oisinoc89@gmail.com**; patrick.mcevoy@dit.ie; max.ammann@dit.ie).

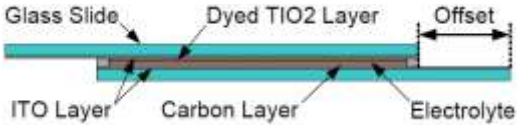

Fig. 2 – Dye-Sensitised Solar Cell Structure

TABLE I
SOLAR CELL MATERIAL PROPERTIES

Material	Dielectric Constant	Conductivity	Reference
Glass Slide	6.7	N/A	11
ITO	N/A	10^{-6} S/m	12
TiO_2	85	N/A	13
Electrolyte	N/A	3×10^{-4} S/m	14
Silicon Sealant	2.8	2.5×10^{-14} S/m	15

II. DYE-SENSITISED SOLAR CELL MANUFACTURE

The DS-cell comprised two transparent electrodes made from 2 mm thick glass slides with a thin conductive layer of ITO, shown in Fig. 2. A layer of TiO_2 was sintered to one slide to establish the anode and dye molecules were added to enable the TiO_2 to absorb energy from visible light. The opposite slide was coated with carbon (C) to make the cathode. Silicon glue was used to seal three sides between the electrode slides, with their separation controlled with temporary 0.4 mm thick acrylic shims. With removal of the shims, an electrolyte for charge transport was poured between the slides and the cell was sealed. Four DS-cells were made with materials referenced in Table I. Conductive copper tape connected the printed copper balun to the ITO-doped glass.

III. RESULTS AND DISCUSSION

A 1,450 lx tungsten halogen directed light source was located 960 mm from the solar cell to evaluate the solar power generated. Table II shows short-circuit current (I_{sc}) and open circuit voltages (V_{oc}) for various sample DS-cells and the solar-antenna. Each side of the DS-cells were measured facing the light source at exposure times t = 0 s (cold) and t = 300 s. Considerable variation in V_{oc} and I_{sc} between cells was attributed to broad tolerances due to basic prototyping equipment. The DS-cells produced the highest power when the TiO_2-slide directly faced the light source. The average V_{oc} for the C-slides facing the light source was 18% lower for t = 0 s and 32% lower for t = 300 s. The antenna DS-cells were configured in series so that one TiO_2-slide and one C-slide was exposed to the light source from one side simultaneously.

The DS-cells maximum performances were V_{oc} = 0.744 V and I_{sc} = 22.47 mA/cm^2 with a 71.2% fill factor [8].

TABLE II
MEASURED SOLAR CELL RESULTS

Solar Cell Under Test	Exposed Face	Cold Cell (t = 0 seconds)		Extended Exposure (t = 300 seconds)	
		V_{oc} (V)	I_{sc} (mA)	V_{oc} (V)	I_{sc} (mA)
Solar Cell 1	TiO_2	0.328	0.055	0.245	0.049
Solar Cell 1	Carbon	0.270	0.015	0.165	0.012
Solar Cell 2	TiO_2	0.351	0.101	0.258	0.091
Solar Cell 2	Carbon	0.285	0.028	0.177	0.020
Solar Cell 3	TiO_2	0.342	0.100	0.251	0.083
Solar Cell 3	Carbon	0.281	0.025	0.166	0.017
Solar Cell 4	TiO_2	0.326	0.050	0.240	0.046
Solar Cell 4	Carbon	0.270	0.014	0.166	0.011
Solar Antenna	Both	0.565	0.034	0.410	0.034
Solar Antenna	Both	0.502	0.035	0.405	0.028

TABLE III
MEASURED AND SIMULATED ANTENNA PERFORMANCE

Antenna	Frequency (GHz)	Bandwidth (%)	Efficiency (%)	Boresight Gain (dBi)
Measured Copper	1.32	21.2		1.0
Simulated Copper	1.31	23.9	89	1.2
Measured ITO Slide	1.24	26.3		-1.9
Simulated ITO Slide	1.21	25.7	41	-1.9
Measured ITO + TiO_2	1.19	24.3		-2.1
Simulated ITO + TiO_2	1.21	26.8	42	-1.9
Measured Full Cell	1.11	29.1		-1.5
Simulated Full Cell	1.08	27.8	44	-1.5

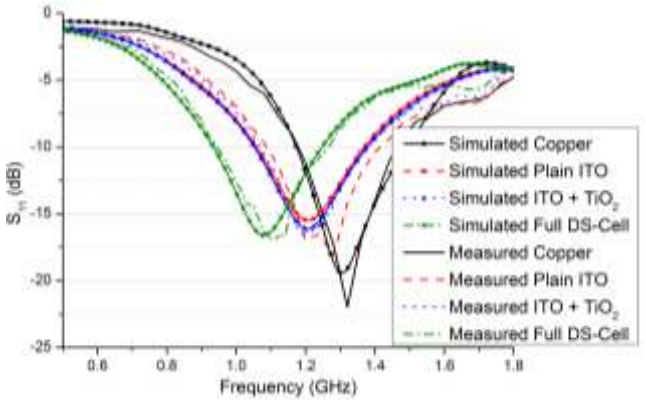

Fig. 3 – Measured and Simulated S_{11} Results

At maximum values, the DS-cell dipole would produce circa 278 mW, which would be adequate to power a Tyndall Mote wireless sensor with an average consumption of 133 µW [16].

Table III summarises the measured and simulated antenna performance results and Fig. 3 shows the S_{11} plots. In order to analyse how the DS-cell components impacted the antenna radiation, various sub-assemblies were assessed. The ITO antenna had 48% reduced efficiency at a lower resonant frequency of 1.24 GHz due to a combination of the 86% higher glass dielectric constant compared to FR4 and the 98% lower ITO conductivity compared to copper. Addition of the higher dielectric TiO_2 had minimal impact on the antenna radiation since current flow was predominantly on the periphery of the glass. Adding the rear glass slide lowered the frequency further to 1.11 GHz due to x-axis offsets between the slide pairs. The offsets exposed the ITO electrical contacts of the antenna and tuned the resonant frequency while taking account of the effective area of the solar cell and solar output power. Additional bandwidth widening was attributed to losses in the rear glass slide.

TABLE IV
MEASURED SOLAR CELL RESULTS

	ITO σ (S/m) × 10^5	Glass ε_r	TiO_2 ε_r	Si ε_r	Si σ (S/m) × 10^{-14}	Electrolyte σ (S/m) × 10^{-4}
A	10	6.7	n/a	n/a	n/a	n/a
B	5	6.7	n/a	n/a	n/a	n/a
C	20	6.7	n/a	n/a	n/a	n/a
D	10	4.0	n/a	n/a	n/a	n/a
E	10	10	n/a	n/a	n/a	n/a
F	10	6.7	85	n/a	n/a	n/a
G	10	6.7	10	n/a	n/a	n/a
H	10	6.7	45	n/a	n/a	n/a
I	10	6.7	85	2.8	2.5	3
J	10	6.7	85	2.3	2.5	3
K	10	6.7	85	3.3	2.5	3
L	10	6.7	85	2.8	1.0	3
M	10	6.7	85	2.8	6.1	3
N	10	6.7	85	2.8	2.5	2
O	10	6.7	85	2.8	2.5	4

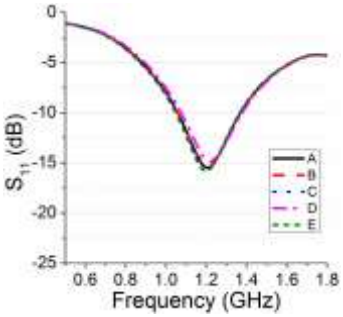

Fig. 4 – Reflection Coefficient Variation of ITO Antenna

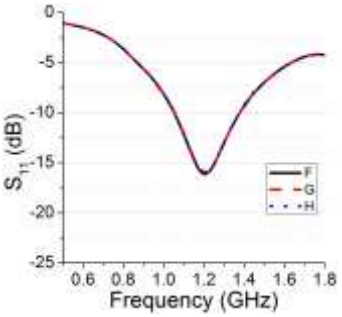

Fig. 5 – Reflection Coefficient Variation of ITO + TiO_2 Antenna

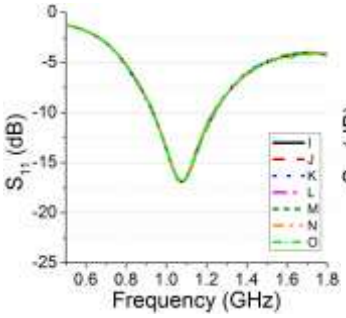

Fig. 6 – Reflection Coefficient Variation of Full Solar Antenna

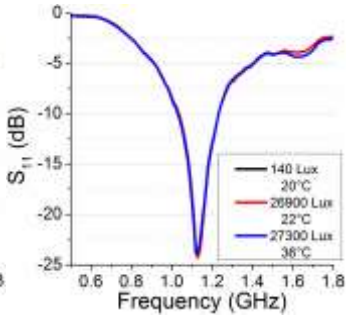

Fig. 7 – Full Solar Antenna S_{11} for Different Insolation Levels

Simulated analyses of the range of material properties of the DS-cell components are shown in Table IV. The ITO antenna was used to investigate the dielectric constant of the glass and the conductivity of the ITO layer. Fig. 4 showed that the typical $5 \le \sigma \le 20$ ($\times 10^5$) range of ITO conductivity was immaterial to the antenna performance. A 4 to 10 increase of the dielectric constant of the glass lowered the resonant frequency by 7.5 MHz and widened the bandwidth by 6 MHz.

The ITO + TiO_2 antenna assessed the effects of varying the TiO_2 dielectric constant, shown in Fig. 5. For a typical TiO_2 dielectric constant $10 \le \varepsilon_r \le 85$ range, the impact on the antenna performance was negligible due to the offset from the main current path.

The fully assembled DS-cell antenna assessed the effects of varying the dielectric constant and conductance of the silicon sealant and the conductance of the electrolyte. Fig. 6 showed that these materials have minimal impact on the antenna performance. The S_{11} for the DS-cell antenna was also

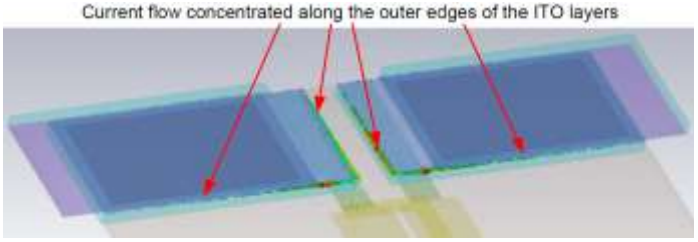

Fig. 8 – Current Flow on Full Solar Antenna

measured under various levels of insolation. Measured light intensity was 140 lx and cell surface temperature was 20 °C with the light off. With the light on for a few seconds, the light intensity was 26,900 lx and the surface temperature was 22 °C. At t = 300 s with the light on, the light intensity was 27,300 lx and the surface temperature was 36 °C. The measured S_{11} is shown in Fig. 7. No significant variation was observed between the light source being turned on or following t = 300 s exposure. Variation between Fig. 3 and Fig. 7 was attributed to the confined test area of the solar test facility which was not designed for antenna testing.

Inspection of the simulated surface currents on material layers revealed current densities below 1 A/m in the TiO_2 layers, electrolyte and silicon sealant, as shown in Fig. 8. This suggested that the two ITO slides couple capacitively and a simulation of the DS-cell antenna without these materials confirmed this. The complete removal of these materials produced a limited downward frequency shift of 5 MHz and a bandwidth reduction of 4.6 MHz.

There were three possible DS-cell configurations in the completed solar antenna: (a) One TiO_2-slide and one C-slide connected to the balun; (b) both C-slides connected to the balun, and (c) both TiO_2-slides connected to the balun. Configuration (a) was manufactured for a higher output voltage and easier power management. Simulations of configurations (b) and (c) demonstrated an insignificant 0.5 MHz frequency shift without bandwidth or radiation pattern changes.

The measured *xy*-plane beamwidths for the antenna were 86°, 84°, 89° and 86° for the Copper, ITO, ITO + TiO_2 and complete solar antenna, respectively. Similarly, the measured *yz*-plane beamwidths for the antenna were 360°, 307°, 308° and 360°, respectively. Large beamwidths are essential for a

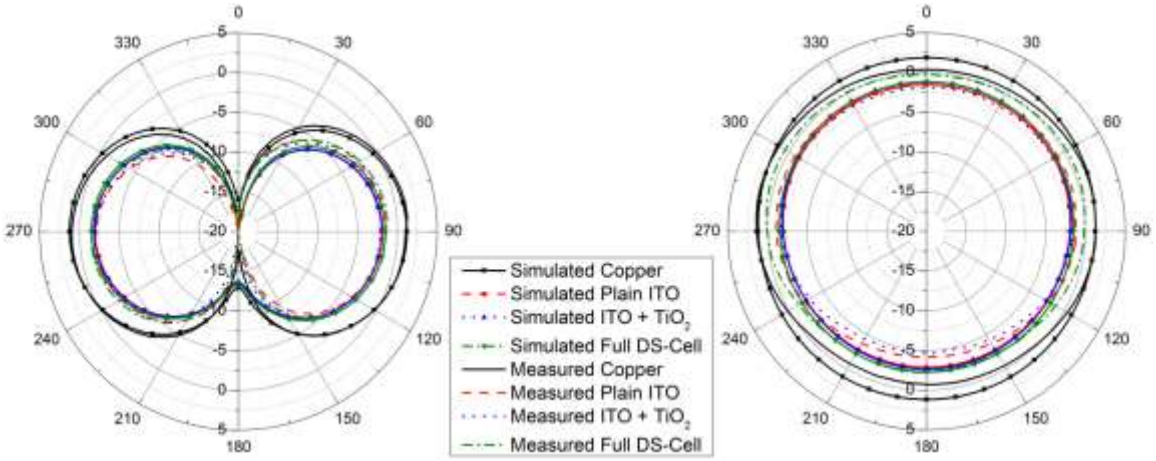

Fig. 9 – Radiation Pattern XY (left) and YZ (right)

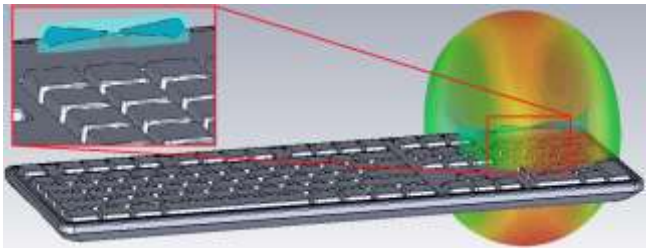

Fig. 10 – Flexible Transparent Bow-Tie Dipole

solar antenna to ensure that the antenna can be setup to maximise both solar insolation and the wireless link. Radiations patterns are shown in Fig. 9.

The antennas with ITO on glass slides had a 3 dBi boresight gain reduction compared to the copper dipole due to reduced conductivity of the ITO layer and greater loss in the glass.

IV. Envisaged Application

With more advanced manufacturing technology, it is anticipated that Polyethylene Naphthalate (PEN) packing would reduce complex material losses. Additionally, the ITO, TiO2 layers and electrolyte could be sintered and packaged using proprietary shapes for more targeted design frequencies, reduced dimensions and feed options. Fig. 10 illustrates a simulated model of a desired compact DS-cell bow-tie dipole antenna on 0.2 mm thick PEN substrate, $\varepsilon_r = 3.2$. A CST Microwave Studio © genetic algorithm optimiser was used to refine the bow-tie elements comprising an isosceles trapezoid and a spline curve. The 19.51 mm leg trapezoids had bases of 0.78 mm and 6.75 mm. The spline curve centre point extended by 1.88 mm. Fig. 11 shows simulated S_{11} for 2.25-2.57 GHz.

The flexible DS-cell antenna was modelled perpendicular to a wireless keyboard to accept light insolation from both faces in order to power the keyboard while enabling a wireless link. Typically, a wireless keyboard requires a 1.5 V battery and draws 3 mA when active. Based on optimum V_{OC}/I_{SC} DS-cell values [8], series-connected DS-cells could produce 1.49 V and 15.5 mA, which would be more than adequate power.

V. Conclusions

This paper reports the first dye-sensitised solar cell antenna in a proof-of-concept dipole configuration as a feasibility study of various circuit configurations of the DS-cell.

The toroidal radiation pattern was not subject to the anisotropy and coupling with metallic components that are part of silicon solar cells. The material properties of the sub-parts of the DS-cell were examined to study impacts on the radiated performance. Comprised of glass packaging and silicon sealant, simulated models of the prototype solar antenna indicted that glass dominated the electromagnetic loading while other materials had negligible effects.

Although the prototype DS-cell antenna had a limited 19 µW power output, more specialised laboratories could exploit advanced manufacturing processes to reduce impurities, improve TiO_2 layer uniformity, accurate electrode spacing and utilize dyes which are more sensitive to the solar spectrum to yield a ~278 mW output from the same footprint.

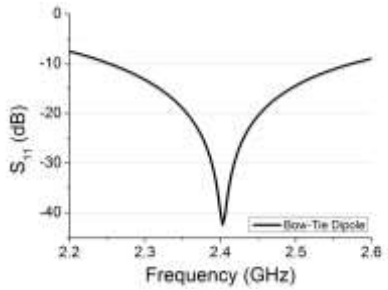

Fig. 11 – Simulated Bow-Tie Dipole S_{11}

An omnidirectional pattern in the *yz*-plane enables greater probability of maintaining a wireless link on portable devices, for example wireless keyboards or remote sensors. For indoor use, it is envisaged that DS-cell antennas will outperform both crystalline- and amorphous- silicon antennas in terms of volume size and energy absorption from diffuse light.

References

[1] M. Danesh, J.R. Long, "An Autonomous Wireless Sensor Node Incorporating a Solar Cell Antenna for Energy Harvesting", *IEEE Transactions on Microwave Theory and Techniques*, vol. 59, no. 12, pp. 3546-3555, 2011.

[2] O. O'Conchubhair, A. Narbudowicz, P. McEvoy, M.J. Ammann, "Circularly polarised solar antenna for airborne communication nodes", *Electronics Letters*, vol.51, no. 9, pp. 667-669, 2015.

[3] D. Wei, "Dye Sensitized Solar Cells" *International Journal of Molecular Sciences*, vol. 11, no. 3, pp. 1103-1113, 2010.

[4] T. Miyasaka, T.N> Murakami, "The photocapacitor: An efficient self-charging capacitor for direct storage of solar energy" *Applied Physics Letters*, vol. 85, no. 17, pp. 3932-3934, Oct. 2004.

[5] S.V. Shynu, M.J. Roo Ons, G. Ruvio, M.J. Ammann, S. McCormack, B. Norton, "A microstrip printed dipole solar antenna using polycrystalline silicon solar cells" *Antennas and Propagation Society International Symposium*, 5-11 July 2008.

[6] S.V. Shynu, M.J. Ammann, S.J. McCormack, B. Norton, "Emitter-wrap-through photovoltaic dipole antenna with solar concentrator" *Electron. Lett.* vol. 45, no. 5, pp. 241-242, 2009.

[7] M. Danesh, J. R. Long, "Photovoltaic Antennas for Autonomous Wireless Systems" *IEEE Transactions on Circuits and Systems*, vol. 58, pp. 807-811, 2011.

[8] M.A. Green, K. Emery, Y. Hishikawa, W. Warta, E.D. Dunlop, "Solar cell efficiency tables (version 47)" *Progress in Photovoltaics: Research and Applications*, vol. 24, no. 1, Nov. 2015.

[9] S. V. Shynu, M. J. Roo Ons, P. McEvoy, M. J. Ammann, S. J. McCormack, B. Norton, "Integration of Microstrip Patch Antenna with Polycrystalline Silicon Solar Cell" *IEEE Transactions on Antennas and Propagation*, vol.57, no.12, pp.3969-3972, Dec. 2009.

[10] S. Vaccaro, J.R. Mosig, P. de Maagt, "Two advanced solar antenna "SOLANT" designs for satellite and terrestrial communications," *IEEE Transactions on Antennas and Propagation*, vol.51, no.8, pp.2028-2034, Aug. 2003.

[11] Schott AG, "D 263® T Thin Glass" D 263 datasheet, May. 2013.

[12] "Material: Indium Tin Oxide (ITO)", *mit.edu*. [online]. Available: http://www.mit.edu/~6.777/matprops/ito.htm. [Accessed: May. 11, 2015].

[13] L.Q. Zhu, L.D. Zhang, Q. Fang, "X-ray photoelectron spectroscopy study of ZrO_2/TiO_2/Si stack", *Applied Physics Letters*, vol. 91, no. 17, Oct. 2007.

[14] V. Jovanovski, E. Stathatos, B. Orel, P. Lianos, "Dye-sensitized solar cells with electrolyte based on a trimethoxysilane-derived ionic liquid" *Thin Solid Films*, vol. 511, pp. 634-637, July 2006.

[15] GE Silicones, *GE Silicones RTV120 Series Neutral Cure Adhesive Sealant*.

[16] W.S. Wang, T. O'Donnell, L. Ribetto, B. O'Flynn, M. Hayes, C. O'Mathuna, "Energy harvesting embedded wireless sensor system for building environment applications" *1st Intern. Conf. Wireless Communication, Vehicular Technology, Information Theory and Aerospace & Electronic Systems Technol.*, pp.36-41, 17-20 May 2009.